Study for the Pentaquark Potential in SU(3) Lattice QCD

Fumiko Okiharu

Department of Physics, Nihon University, 1-8-14 Kanda-Surugadai, Chiyoda, Tokyo 101-8308, Japan

Hideo Suganuma

Faculty of Science, Tokyo Institute of Technology, 2-12-1 Ohokayama, Tokyo 152-8551, Japan

Toru T. Takahashi

Yukawa Institute for Theoretical Physics, Kyoto University, Kitashirakawa, Sakyo, Kyoto 606-8502, Japan
(Received 2 July 2004; published 19 May 2005)

We perform the first study of the static pentaquark (5Q) potential V_{5Q} in SU(3) quenched lattice QCD with $16^3 \times 32$ and $\beta = 6.0$. From the 5Q Wilson loop, V_{5Q} is calculated in a gauge-invariant manner, with the smearing method to enhance the ground-state component. V_{5Q} is well described by the OGE–plus–multi-Y ansatz: a sum of the one-gluon-exchange (OGE) Coulomb term and the multi-Y-type linear term proportional to the minimal total length of the flux tube linking the five quarks. Comparing with $Q\bar{Q}$ and 3Q potentials, we find a universality of the string tension, $\sigma_{Q\bar{Q}} \simeq \sigma_{3Q} \simeq \sigma_{5Q}$, and the OGE result for Coulomb coefficients.

In 1979, the first application of lattice QCD simulations was done for the interquark potential between a quark and an antiquark using the Wilson loop [1]. Since then, the study of the interquark force has been one of the central issues in lattice QCD. Actually, in hadron physics, the interquark force can be regarded as an elementary quantity to connect the "quark world" to the "hadron world," and it plays an important role in hadron properties. In addition to the $Q\bar{Q}$ potential, recent lattice QCD studies clarify the three-quark (3Q) potential [2], which is responsible to the baryon structure.

Recently, exotic pentaquark (5Q) baryons such as the $\Theta^+(1540)$ ($uudd\bar{s}$), the $\Xi^{--}(1862)$ ($ddss\bar{u}$), and the $\Theta_c(3099)$ ($uudd\bar{c}$) were observed by several experimental groups [3]. These discoveries of multiquark hadrons are expected to reveal new aspects of hadron physics [4–12], especially for the interquark force such as the quark confinement force [7], the color-magnetic interaction, and the diquark correlation [5].

In this Letter, motivated by the recent discovery of the pentaquark baryons, we describe the first study of the static pentaquark (5Q) potential V_{5Q}, i.e., the interquark force in the 5Q system, in lattice QCD. Note that the lattice QCD result of V_{5Q} presents the proper Hamiltonian for the quark-model calculation of the multiquark system [6] based on QCD. In addition, clarifying the confinement potential in the multiquark system is useful also for understanding the confinement mechanism.

For the pentaquark system, we investigate the QQ-$\bar{Q}$-QQ type configuration with the two "QQ clusters" belonging to the $\bar{\mathbf{3}}$ representation of the SU(3) color as shown in Fig. 1, since this type of the 5Q configuration is expected to have less energy and seems to be natural as a realistic candidate of the $\Theta^+(1540)$. Indeed, in the perturbative sense, an attractive (repulsive) force acts between

two quarks, when their total SU(3) color belongs to $\bar{\mathbf{3}}$ ($\mathbf{6}$). Therefore, the nearest QQ cluster tends to form $\bar{\mathbf{3}}$ rather than $\mathbf{6}$ in the low-lying 5Q system, which leads to the $\bar{\mathbf{3}}$-diquark model [5].

Similar to the derivation of the $Q\bar{Q}$ (3Q) potential from the (3Q) Wilson loop, the 5Q static potential V_{5Q} can be calculated with the 5Q Wilson loop W_{5Q}, which is defined in a gauge-invariant manner as shown in Fig. 2.

We define the 5Q Wilson loop W_{5Q} [7] as

$$W_{5Q} \equiv \frac{1}{3!} \epsilon^{abc} \epsilon^{a'b'c'} M^{aa'} (\tilde{L}_3 \tilde{L}_{12} \tilde{L}_4)^{bb'} (\tilde{R}_3 \tilde{R}_{12} \tilde{R}_4)^{cc'}, \quad (1)$$

where $\tilde{M}, \tilde{L}_i, \tilde{R}_i$ ($i = 1, 2, 3, 4$) are given by

$$\tilde{M}, \tilde{L}_i, \tilde{R}_i \equiv P \exp\left\{ ig \int_{M, L_i, R_i} dx^\mu A_\mu(x) \right\} \in \mathrm{SU}(3)_c. \quad (2)$$

As shown in Fig. 2, $\tilde{M}, \tilde{L}_i, \tilde{R}_i$ ($i = 3, 4$) are linelike variables and $\tilde{L}_i, \tilde{R}_i$ ($i = 1, 2$) are staplelike variables. Here, $\tilde{L}_{12}, \tilde{R}_{12}$ are defined as

$$\tilde{L}_{12}^{a'a} \equiv \tfrac{1}{2} \epsilon^{abc} \epsilon^{a'b'c'} \tilde{L}_1^{bb'} \tilde{L}_2^{cc'}, \qquad \tilde{R}_{12}^{a'a} \equiv \tfrac{1}{2} \epsilon^{abc} \epsilon^{a'b'c'} \tilde{R}_1^{bb'} \tilde{R}_2^{cc'}.$$
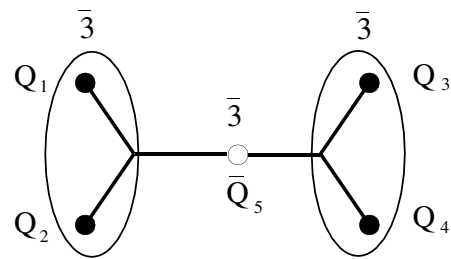$$(3)$$

FIG. 1. The QQ-$\bar{Q}$-QQ type configuration for the pentaquark system. The two QQ clusters belong to the $\bar{\mathbf{3}}$ representation of the color SU(3).
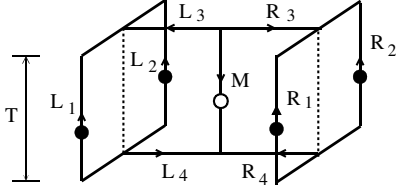
FIG. 2. The pentaquark ($5Q$) Wilson loop W_{5Q} for the $5Q$ potential V_{5Q}. The contours M, L_i, R_i ($i = 3, 4$) are linelike and L_i, R_i ($i = 1, 2$) are staplelike. The $5Q$ gauge-invariant state is generated at $t = 0$ and is annihilated at $t = T$ with the five quarks ($4Q$-$\bar{Q}$) being spatially fixed in $\mathbf{R}^3$ for $0 < t < T$.

Note that the $5Q$ Wilson loop W_{5Q} is gauge invariant, and its gauge invariance is owing to the nontrivial assignment of the color indices of $\tilde{L}_{12}$ and $\tilde{R}_{12}$ in Eq. (3). (Recall that "two quark lines" combining into $\bar{3}$-representation correspond to an "antiquark line" as the color current.)

In principle, the ground-state $5Q$ potential V_{5Q} is obtained from the $5Q$ Wilson loop $\langle W_{5Q} \rangle$ as $V_{5Q} = -\lim_{T \to \infty} \frac{1}{T} \ln \langle W_{5Q} \rangle$. In practice, for the accurate lattice calculation of V_{5Q} with finite T, we use the gauge-covariant smearing method [2] to enhance the ground-state component of the $5Q$ state in the $5Q$ Wilson loop. The smearing is a powerful method for the accurate calculation of the $Q\bar{Q}$ and the $3Q$ potentials [2], and is expressed as the iterative replacement of the spatial link variables $U_i(s)$ ($i = 1, 2, 3$) by the obscured link variables $\bar{U}_i(s) \in SU(3)_c$ which maximizes $\mathrm{Re\, tr}\{\bar{U}_i^\dagger(s) V_i(s)\}$ with $V_i(s) \equiv \alpha U_i(s) + \sum_{j \neq i} \sum_{\pm} \{U_{\pm j}(s) U_i(s \pm \hat{j}) U_{\pm j}^\dagger(s + \hat{i})\}$ with the simplified notation of $U_{-j} \equiv U_j^\dagger(s - \hat{j})$. We here adopt $\alpha = 2.3$ and the iteration number $N_{\mathrm{smr}} = 40$, which lead to a large enhancement of the ground-state component in the $5Q$ Wilson loop at $\beta = 6.0$.

Now, we proceed to the actual lattice QCD calculation for the $5Q$ potential V_{5Q} [7]. We generate 150 gauge configurations using $SU(3)_c$ lattice QCD with the standard action with $\beta = 6.0$ and $16^3 \times 32$ at the quenched level. The gauge configurations are taken every 500 sweeps after a thermalization of 5000 sweeps using the pseudo-heat-bath algorithm. The lattice spacing a is estimated as $a \simeq 0.104$ fm from the string tension $\sigma = 0.89$ GeV/fm in the $Q\bar{Q}$ potential $V_{Q\bar{Q}}$ [7].

As for the $5Q$ configuration, we consider the QQ-$\bar{Q}$-QQ type configuration as shown in Fig. 1. Note that the multi-quark system including four or more quarks can take a three-dimensional shape, while the $Q\bar{Q}$ and the $3Q$ systems can take only planar configuration [7,11]. Then we investigate both the planar and the twisted $5Q$ configurations as shown in Figs. 3 and 4, respectively.

For these types of $5Q$ configurations, we calculate the $5Q$ potential V_{5Q} from the $5Q$ Wilson loop $\langle W_{5Q} \rangle$ using the smearing method. Owing to the smearing, the ground-state component is largely enhanced, and therefore the $5Q$ Wilson loop $\langle W_{5Q} \rangle$ composed with the smeared link variable exhibits a single-exponential behavior as $\langle W_{5Q} \rangle \simeq$
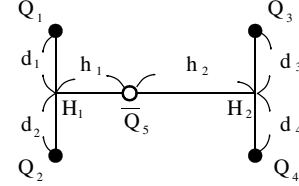

FIG. 3. A planar $5Q$ configuration. $Q_1 Q_2$ is parallel to $Q_3 Q_4$, and $H_1 H_2$ is perpendicular to $Q_1 Q_2$ and $Q_3 Q_4$.

$e^{-V_{5Q}T}$ even for a small value of T. Then, for each $5Q$ configuration, we extract V_{5Q} from the least squares fit with the single-exponential form

$$\langle W_{5Q} \rangle = \bar{C} e^{-V_{5Q}T} \tag{4}$$

in the range of $T_{\min} \leq T \leq T_{\max}$ listed in Table I. The prefactor $\bar{C}$ physically means the ground-state overlap, and $\bar{C} \simeq 1$ corresponds to the quasi ground state. Here, we choose the fit range of T such that the stability of the "effective mass" $V(T) \equiv \ln\{\langle W_{5Q}(T) \rangle / \langle W_{5Q}(T + 1) \rangle\}$ is observed in the range of $T_{\min} \leq T \leq T_{\max} - 1$. For the lattice calculation of $\langle W_{5Q} \rangle$, we use the translational and the rotational symmetries on lattices.

Here, we take $d_1 = d_2 = d_3 = d_4 \equiv d$, and present the lattice QCD result of V_{5Q} in terms of (d, h_1, h_2). For 56 different patterns of the $5Q$ configurations as shown in Figs. 3 and 4, we present the lattice QCD data for the $5Q$ potential V_{5Q} together with the ground-state overlap $\bar{C}$ in Tables I and II. The statistical errors are estimated with the jackknife method. We find a large ground-state overlap as $\bar{C} > 0.85$ for almost all $5Q$ configurations.

Next, we consider the theoretical form of the $5Q$ potential V_{5Q}. The lattice QCD studies [2] at the quenched level show that the $Q\bar{Q}$ potential $V_{Q\bar{Q}}$ takes the form of

$$V_{Q\bar{Q}}(r) = -\frac{A_{Q\bar{Q}}}{r} + \sigma_{Q\bar{Q}} r + C_{Q\bar{Q}}, \tag{5}$$

and the $3Q$ potential V_{3Q} takes the form of

$$V_{3Q} = -A_{3Q} \sum_{i<j} \frac{1}{|\mathbf{r}_i - \mathbf{r}_j|} + \sigma_{3Q} L_{\min} + C_{3Q}, \tag{6}$$

where $L_{\min}$ denotes the minimal total length of color flux tubes linking the three quarks. In fact, both $V_{Q\bar{Q}}$ and V_{3Q} are described by a sum of the one-gluon-exchange (OGE) result and the long-distance flux-tube result [2,13].

For the static pentaquark ($5Q$) system, we find that the lattice QCD results are well described by the OGE plus
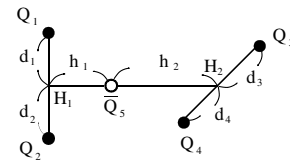

FIG. 4. A twisted $5Q$ configuration. $Q_1 Q_2$ is perpendicular to $Q_3 Q_4$, and $H_1 H_2$ is perpendicular to $Q_1 Q_2$ and $Q_3 Q_4$.

TABLE I. Lattice QCD results for the pentaquark potential V_{5Q} for the planar $5Q$ configuration labeled by (d, h_1, h_2) as shown in Fig. 3. We list also the ground-state overlap $\bar{C}$, the fit range of T, and the theoretical form V_{5Q}^{theor} of the OGE plus multi-Y ansatz (7) with (A_{5Q}, σ_{5Q}) fixed to be (A_{3Q}, σ_{3Q}) in V_{3Q} in Ref. [2]. All the data are measured in the lattice unit.

(d, h_1, h_2)	V_{5Q}	$\bar{C}$	T_{min}-T_{max}	V_{5Q}^{theor}
(1, 1, 1)	1.4452(11)	0.9539(21)	2-7	1.4433
(1, 1, 2)	1.5409(13)	0.9506(25)	2-8	1.5414
(1, 1, 3)	1.6177(19)	0.9512(33)	2-7	1.6146
(1, 1, 4)	1.6793(20)	0.9431(35)	2-7	1.6767
(1, 1, 5)	1.7381(23)	0.9394(40)	2-6	1.7332
(1, 1, 6)	1.7918(28)	0.9311(49)	2-6	1.7866
(1, 1, 7)	1.8441(31)	0.9232(56)	2-6	1.8380
(1, 2, 2)	1.6314(17)	0.9503(29)	2-6	1.6322
(1, 2, 3)	1.7011(20)	0.9427(34)	2-5	1.7021
(1, 2, 4)	1.7680(25)	0.9478(43)	2-6	1.7623
(1, 2, 5)	1.8190(29)	0.9297(50)	2-6	1.8177
(1, 2, 6)	1.8717(33)	0.9205(57)	2-5	1.8704
(1, 3, 3)	1.7723(24)	0.9405(39)	2-4	1.7702
(1, 3, 4)	1.8336(28)	0.9351(49)	2-7	1.8293
(1, 3, 5)	1.8913(33)	0.9320(62)	2-5	1.8839
(1, 4, 4)	1.8939(31)	0.9293(53)	2-4	1.8877
(2, 1, 1)	1.7531(23)	0.9393(40)	2-5	1.7515
(2, 2, 2)	1.8803(31)	0.9292(54)	2-6	1.8887
(2, 3, 3)	2.0030(37)	0.9284(64)	2-5	2.0098
(2, 4, 4)	2.1122(49)	0.9116(91)	2-5	2.1211
(3, 1, 1)	1.9734(37)	0.9138(66)	2-5	1.9850
(3, 2, 2)	2.0811(45)	0.9070(75)	2-5	2.0942
(3, 3, 3)	2.1886(53)	0.9003(92)	2-4	2.2047
(3, 4, 4)	2.3043(68)	0.9084(113)	2-5	2.3105
(4, 1, 1)	2.1697(60)	0.8948(100)	2-5	2.1958
(4, 2, 2)	2.2734(60)	0.8890(100)	2-5	2.2829
(4, 3, 3)	2.3657(73)	0.8606(120)	2-4	2.3864
(4, 4, 4)	2.4706(104)	0.8534(164)	2-5	2.4884

TABLE II. Lattice QCD results for the pentaquark potential V_{5Q} for the twisted $5Q$ configuration labeled by (d, h_1, h_2) as shown in Fig. 4. The notations are the same in Table I.

(d, h_1, h_2)	V_{5Q}	$\bar{C}$	T_{min}-T_{max}	V_{5Q}^{theor}
(1, 1, 1)	1.4476(23)	0.9378(64)	3-8	1.4458
(1, 1, 2)	1.5438(14)	0.9528(25)	2-8	1.5419
(1, 1, 3)	1.6155(17)	0.9459(31)	2-6	1.6148
(1, 1, 4)	1.6767(21)	0.9370(37)	2-6	1.6767
(1, 1, 5)	1.7365(22)	0.9357(42)	2-5	1.7332
(1, 1, 6)	1.7912(26)	0.9297(42)	2-4	1.7866
(1, 1, 7)	1.8337(88)	0.8933(231)	3-5	1.8380
(1, 2, 2)	1.6302(16)	0.9472(29)	2-8	1.6324
(1, 2, 3)	1.7022(18)	0.9445(32)	2-4	1.7022
(1, 2, 4)	1.7657(25)	0.9427(44)	2-5	1.7624
(1, 2, 5)	1.8232(30)	0.9385(51)	2-7	1.8177
(1, 2, 6)	1.8728(32)	0.9230(58)	2-8	1.8704
(1, 3, 3)	1.7710(24)	0.9376(42)	2-6	1.7702
(1, 3, 4)	1.8326(27)	0.9335(46)	2-4	1.8293
(1, 3, 5)	1.8952(32)	0.9394(58)	2-7	1.8839
(1, 4, 4)	1.8950(30)	0.9315(52)	2-4	1.8877
(2, 1, 1)	1.7735(23)	0.9377(41)	2-6	1.7615
(2, 2, 2)	1.8832(30)	0.9279(54)	2-7	1.8899
(2, 3, 3)	2.0011(37)	0.9233(64)	2-5	2.0100
(2, 4, 4)	2.1155(49)	0.9167(85)	2-6	2.1212
(3, 1, 1)	2.0049(37)	0.9032(67)	2-5	2.0008
(3, 2, 2)	2.0873(38)	0.8987(69)	2-4	2.0973
(3, 3, 3)	2.1870(54)	0.8912(92)	2-6	2.2055
(3, 4, 4)	2.3021(68)	0.9019(113)	2-5	2.3108
(4, 1, 1)	2.2141(65)	0.8741(107)	2-6	2.2155
(4, 2, 2)	2.2874(64)	0.8768(107)	2-5	2.2879
(4, 3, 3)	2.3715(70)	0.8577(118)	2-4	2.3880
(4, 4, 4)	2.4680(94)	0.8459(149)	2-4	2.4890

multi-Y ansatz: a sum of the OGE Coulomb term, and the multi-Y-type linear term [7],

$$V_{5Q} = \frac{g^2}{4\pi} \sum_{i<j} \frac{T_i^a T_j^a}{|\mathbf{r}_i - \mathbf{r}_j|} + \sigma_{5Q} L_{min} + C_{5Q}$$
$$= -A_{5Q}\left\{\left(\frac{1}{r_{12}} + \frac{1}{r_{34}}\right) + \frac{1}{2}\left(\frac{1}{r_{15}} + \frac{1}{r_{25}} + \frac{1}{r_{35}} + \frac{1}{r_{45}}\right)\right.$$
$$\left. + \frac{1}{4}\left(\frac{1}{r_{13}} + \frac{1}{r_{14}} + \frac{1}{r_{23}} + \frac{1}{r_{24}}\right)\right\} + \sigma_{5Q} L_{min} + C_{5Q}, \quad (7)$$

with $r_{ij} \equiv |\mathbf{r}_i - \mathbf{r}_j|$ and the ith quark location $\mathbf{r}_i$ in Fig. 1.

Here, L_{min} is the minimal length of the flux tube linking the five quarks. For the $5Q$ system, L_{min} is the length of the multi-Y-shaped flux tube as shown in Fig. 1, unless h_i ($i = 1, 2$) is rather small compared with d_j ($j = 1, 2, 3, 4$). (For an extreme case, e.g., $d > \sqrt{3}h_1$, we assume that the flux tube is formed as the two straight lines on $Q_1 Q_5$ and $Q_2 Q_5$, considering the color combination [14].)

We explain L_{min} for the $5Q$ configuration as shown in Figs. 3 and 4 with $d_1 = d_2 = d_3 = d_4 \equiv d$ and $h \equiv h_1 + h_2$. In the case of $h \geq \frac{2}{\sqrt{3}}d$, the $5Q$ system takes a double-Y-shaped flux tube, and the minimal value of the total flux-tube length is expressed as $L_{min} = h + 2\sqrt{3}d$. In the case of $h \leq \frac{2}{\sqrt{3}}d$, the $5Q$ system takes an X-shaped flux tube with $L_{min} = 2\sqrt{h^2 + 4d^2}$.

Note that there appear three kinds of Coulomb coefficients $(A_{5Q}, \frac{1}{2}A_{5Q}, \frac{1}{4}A_{5Q})$ in the pentaquark system, while only one Coulomb coefficient, $A_{Q\bar{Q}}$ or A_{3Q}, appears in the $Q\bar{Q}$ or the $3Q$ system. Here, A_{5Q} in Eq. (7) corresponds to A_{3Q} or $\frac{1}{2}A_{Q\bar{Q}}$ in terms of the OGE result.

We add in Tables I and II the theoretical form V_{5Q}^{theor} of the OGE plus multi-Y ansatz (7) with (A_{5Q}, σ_{5Q}) fixed to be (A_{3Q}, σ_{3Q}) in the $3Q$ potential V_{3Q} obtained in Ref. [2]; i.e., $A_{5Q} = A_{3Q} \simeq 0.1366$, $\sigma_{5Q} = \sigma_{3Q} \simeq 0.046a^{-2}$, and $C_{5Q} \simeq 1.58a^{-1}$. (Note that there is no adjustable parameter for the theoretical form V_{5Q}^{theor} besides an irrelevant constant C_{5Q}, since A_{5Q} and σ_{5Q} are fixed to be A_{3Q} and σ_{3Q}, respectively.) Thus, the $5Q$ potential V_{5Q} is found to be well described by the OGE Coulomb plus the multi-Y-type linear potential.

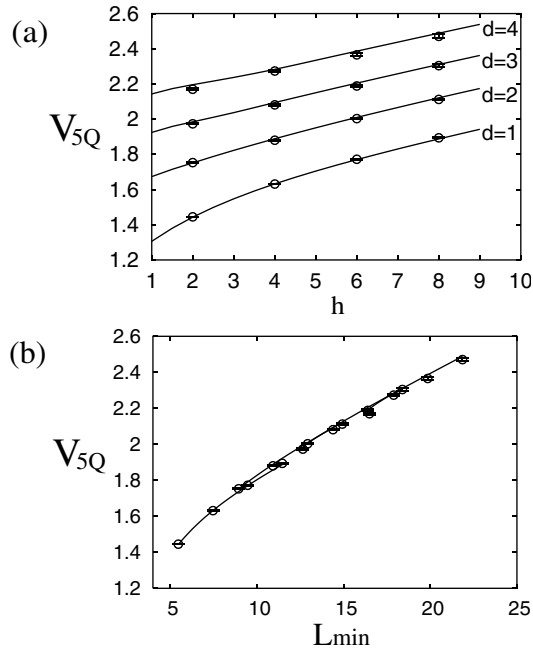P H Y S I C A L   R E V I E W   L E T T E R S

(a)

(b)

FIG. 5. Lattice QCD results of the pentaquark potential V_{5Q} for the planar $5Q$ configuration with $h_1 = h_2 \equiv h/2$ in Fig. 3: (a) V_{5Q} plotted against (d, h); (b) V_{5Q} vs L_{min}. The symbols denote the lattice data, and the curves the theoretical form of the OGE plus multi-Y ansatz in the lattice unit.

We show in Fig. 5 typical examples of the lattice QCD data for the pentaquark potential V_{5Q}. The symbols denote the lattice data, and the curves denote the theoretical form of the OGE plus multi-Y ansatz with (A_{5Q}, σ_{5Q}) fixed to be (A_{3Q}, σ_{3Q}). One finds a good agreement between the lattice QCD data and the theoretical curves.

On the confinement force, as shown in Fig. 5(b), V_{5Q} becomes a (single-valued) linear function of L_{min} at large distances, which indicates that the long-distance force is genuinely five-body and the flux tube is multi-Y shaped.

Note that the planar and the twisted $5Q$ configurations with the same (d, h_1, h_2) are almost degenerate, although the energy of the planar one is slightly smaller. In terms of the OGE plus multi-Y ansatz, the only energy difference between the two states comes from a small difference of the Coulomb interaction between Q_i ($i = 1, 2$) and Q_j ($j = 3, 4$), where the Coulomb coefficient is reduced as $\frac{1}{4}A_{5Q}$ ($\simeq \frac{1}{8}A_{Q\bar{Q}}$). Then, no special configuration is favored in the $5Q$ system in terms of the energy. This fact also indicates that the $5Q$ system is unstable against the twisted motion of the two QQ clusters as shown in Fig. 4. In fact, general $5Q$ systems tend to take a three-dimensional configuration [7,11] in terms of the entropy.

We have also investigated asymmetric $5Q$ configurations with various different values of d_j and h_i in both planar and twisted cases, and have confirmed the OGE plus multi-Y ansatz for various $5Q$ configurations [14].

From the comparison with the $Q\bar{Q}$ and the $3Q$ potentials, we find the universality of the string tension and the OGE result among $Q\bar{Q}$, $3Q$, and $5Q$ systems as

$$\sigma_{Q\bar{Q}} \simeq \sigma_{3Q} \simeq \sigma_{5Q}, \qquad \tfrac{1}{2}A_{Q\bar{Q}} \simeq A_{3Q} \simeq A_{5Q}. \qquad (8)$$

This result supports the flux-tube picture on the confinement mechanism even for the multiquark system [7].

For further confirmation of the multi-Y-shaped flux-tube formation, it is interesting to measure the action density in the presence of the static five quarks on lattice, as was recently done for the $3Q$ system [13]. For more realistic calculations, full QCD studies are also desired.

To conclude, we have performed the first study of the pentaquark potential in lattice QCD, and have found that the $5Q$ potential is well reproduced by the OGE Coulomb plus multi-Y-type linear potential.

[1] M. Creutz, Phys. Rev. Lett. **43**, 553 (1979); **43**, 890(E) (1979); Phys. Rev. D **21**, 2308 (1980).

[2] T. T. Takahashi *et al.*, Phys. Rev. Lett. **86**, 18 (2001); Phys. Rev. D **65**, 114509 (2002); Phys. Rev. Lett. **90**, 182001 (2003); Phys. Rev. D **70**, 074506 (2004).

[3] T. Nakano *et al.* (LEPS Collaboration), Phys. Rev. Lett. **91**, 012002 (2003); V. V. Barmin *et al.* (DIANA Collaboration), Phys. At. Nucl. **66**, 1715 (2003); S. Stephanyan *et al.* (CLAS Collaboration), Phys. Rev. Lett. **91**, 252001 (2003); J. Barth *et al.* (SAPHIR Collaboration), Phys. Lett. B **572**, 127 (2003); C. Alt *et al.* (NA49 Collaboration), Phys. Rev. Lett. **92**, 042003 (2004); A. Aktas *et al.* (H1 Collaboration), Phys. Lett. B **588**, 17 (2004).

[4] D. Diakonov *et al.*, Z. Phys. A **359**, 305 (1997).

[5] R. L. Jaffe *et al.*, Phys. Rev. Lett. **91**, 232003 (2003).

[6] M. Karliner and H. J. Lipkin, hep-ph/0307243; Phys. Lett. B **575**, 249 (2003).

[7] H. Suganuma *et al.*, in *Proceedings of QCD Down Under, Adelaide, 2004* [Nucl. Phys. B (Proc. Suppl.) 141, 92 (2004)].

[8] S.-L. Zhu, Phys. Rev. Lett. **91**, 232002 (2003); J. Sugiyama, T. Doi, and M. Oka, Phys. Lett. B **581**, 167 (2004).

[9] F. Csikor *et al.*, J. High Energy Phys. 11 (2003) 070.

[10] I. M. Narodetskii *et al.*, Phys. Lett. B **578**, 318 (2004); M. Bando *et al.*, Prog. Theor. Phys. **112**, 325 (2004).

[11] X.-C. Song *et al.*, Mod. Phys. Lett. A **19**, 2791 (2004).

[12] S. L. Zhu, Int. J. Mod. Phys. A **19**, 3439 (2004); M. Oka, Prog. Theor. Phys. **112**, 1 (2004), and references therein.

[13] H. Ichie *et al.*, Nucl. Phys. **A721**, C899 (2003).

[14] F. Okiharu *et al.* (to be published).